

Spectral analysis of electromagnetic emissions from partial discharges in environments with obstacles

Análisis espectral de emisiones electromagnéticas de descargas parciales en entornos con obstáculos

PhD. Jorge Alfredo Ardila Rey ¹, MSc. Daniel Jesús Figueroa Karmelic ¹
MSc. Rodrigo Rozas Valderrama ¹, Ing. Pablo Gaete Morales ¹

¹ Universidad Técnica Federico Santa María, Laboratorio de Investigación y Desarrollo en Alta Tensión (LIDAT), Santiago de Chile 8940000, Departamento de Ingeniería Eléctrica, Chile.

Correspondence: jorge.ardila@usm.cl

Received: July 03, 2024. Accepted: November 14, 2024. Published: January 01, 2025.

How to cite: J. A. Ardila Rey, D. J. Figueroa Karmelic, R. Rozas Valderrama, and P. Gaete Morales, "Spectral analysis of electromagnetic emissions from partial discharges in environments with obstacles", *RCTA*, vol. 1, no. 45, pp. 32–38, Jan. 2025. Recovered from <https://ojs.unipamplona.edu.co/index.php/rcta/article/view/3473>

This work is licensed under a
Creative Commons Attribution-NonCommercial 4.0 International License.



Abstract: The detection of partial discharges (PD) in electrical equipment is essential for assessing the condition of insulation systems. Among existing methods, the measurement of UHF emissions from PD using antennas stands out, as it enables diagnostics in energized installations without requiring a galvanic connection between the sensor and the equipment. This technique offers significant advantages over more traditional methods; however, it is not without challenges. The presence of obstacles in the measurement environment can create destructive and constructive interference by reflecting or diffracting the UHF emissions. These interferences may impact the insulation condition diagnosis, complicate the localization of emission sources, and hinder the identification of the type of PD. This article presents the results of a series of experiments that characterize the effect of various obstacle configurations on the signal recorded by a Vivaldi antenna. The findings identify frequency bands whose amplitude is altered due to constructive interference from waves reflected by the obstacles, providing valuable information to optimize measurements and improve accuracy in PD diagnostics.

Keywords: UHF measurement, metallic obstacles, electromagnetic interference (EMI), partial discharges (PD), electromagnetic emissions (EM).

Resumen: La detección de descargas parciales (DP) en equipos eléctricos es esencial para evaluar el estado de los sistemas de aislamiento. Entre los métodos existentes, la medición de emisiones UHF de PD a través de antenas se destaca por permitir el diagnóstico en instalaciones energizadas sin necesidad de una conexión galvánica entre el sensor y el equipo. Esta técnica presenta ventajas significativas sobre métodos más tradicionales; sin embargo, no está exenta de desafíos. La presencia de obstáculos en el entorno de medición puede generar interferencias destructivas y constructivas, reflejando o difractando las emisiones UHF. Estas interferencias pueden afectar el diagnóstico del estado de la aislación, dificultar la localización del origen de las emisiones y complicar la identificación

del tipo de DP. Este artículo presenta los resultados de una serie de experimentos que caracterizan el efecto de diversas configuraciones de obstáculos en la señal registrada mediante una antena Vivaldi. Los hallazgos permiten identificar las bandas de frecuencia cuya amplitud se ve alterada debido a la interferencia constructiva de ondas reflejadas en los obstáculos, proporcionando información valiosa para optimizar las mediciones y mejorar la precisión en el diagnóstico de DP.

Palabras clave: medición UHF, obstáculos metálicos, interferencia electromagnética (EM), descargas parciales (DP), emisiones electromagnéticas (EM).

1. INTRODUCTION

Partial discharge (PD) monitoring is a fundamental tool for assessing the degradation state of insulation systems in high voltage electrical assets [1], [2]. PD typically occurs in the weakest areas of the insulating material, such as in vacuoles, electrical trees, surface conductive particles and sharp metallic protrusions [3]. This phenomenon progressively degrades the dielectric properties of the material, eventually leading to catastrophic insulation failure. Due to their impulsive nature, PDs generate electromagnetic (EM) emissions over a wide range of frequencies [4]. This allows the use of UHF antennas, which can be strategically placed close to the emission source to detect and monitor the evolution of faults without requiring a galvanic connection to the equipment [5], [6]. In addition to detection, a significant advantage of these sensors is their ability to localize the emitting source by calculating the time difference of arrival (TDOA) of the signals picked up by multiple antennas. However, this localization process faces significant challenges due to interference from external noise sources, such as FM radios, TV broadcasts, WiFi communications and cell phones, which can mask PD emissions in certain frequency bands [7]. Also, the presence of metallic structures such as electrical machine parts, poles, towers and busbars can reflect electromagnetic waves, altering the shape of the pulses detected by the antennas and hindering the accurate calculation of the TDOA [8]-[15].

Changes in the measurement environment, such as the addition or removal of metallic obstacles near the emission source, can induce temporal and spectral variations in the recorded signals. These variations can generate false alarms in UHF monitoring systems, as they can be interpreted as new faults or as the progression of an existing one.

In this paper, the results of an experimental study on the spectral variations experienced by the electromagnetic emissions of two different PD

sources in the presence of obstacles in the measurement environment are presented. The results obtained using a Vivaldi antenna show that, in certain frequency bands, the spectral power can be significantly increased, while in others, noticeable decreases in spectral power are observed. To verify the influence of obstacle grounding, additional experiments were performed keeping the metallic obstacles isolated from ground, observing similar results as in the case with grounded obstacles. Therefore, only the results obtained with grounded obstacles are presented in this work.

2. EXPERIMENTAL SETUP

To characterize the effect of different types of obstacles in the environment of a PD EM emission source during the measurement process, two types of obstacles were designed:

- Metal rectangles of 10 cm x 10 cm and 150 cm in height.
- Metal cylinders of 6.37 cm in diameter and 150 cm in height.

The PD generation and measurement process was carried out using a fully standardized indirect measurement circuit [9]. This circuit was complemented with a commercial PD monitoring system that allowed verifying the presence of PD and the type of source detected. To capture the generated EM emissions, a Vivaldi antenna, operating in broadband from 1.5 GHz, specially designed for UHF PD measurements, was used [10], [16]-[24]. This antenna consists of an exponential slot line or waveguide integrated in a substrate, connected by a microstrip transmission line to an SMA connector.

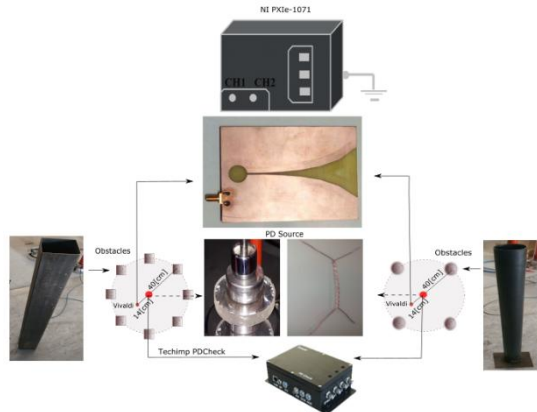


Fig. 1 Experimental configurations based on the different obstacles and PD emission sources.
Source: own elaboration.

The measurement process began, for each test object, by maintaining a low voltage level and a low trigger level in the acquisition system. This allowed the maximum amplitude of the background noise in the laboratory to be established. Subsequently, the trigger level was adjusted above the background noise and the voltage was increased until a stable PD activity was obtained, ensuring that the pulses picked up by the Vivaldi antenna came exclusively from PD sources. Three series of measurements were performed for each test object: the first without obstacles, the second with rectangular obstacles and the third with cylindrical obstacles. During each measurement run, 200 signals were stored with a window of 1 μ s.

The acquisition system used was a PXI high-speed digitizer, with a sampling capacity of 12.5 GS/s, vertical resolution of 8 bits and a bandwidth of 3 GHz. For the measurements reported in this study, the system was set at an acquisition rate of 4 GS/s. As shown in Fig. 1, two obstacle configurations were implemented for each test object. The first configuration consisted of eight rectangular obstacles arranged equidistantly in a circular array around the test object, placed at a distance of 40 cm. The second experimental configuration included six cylindrical obstacles, also placed 40 cm from the PD emission source.

Two different test objects were used to generate stable PD activity in each obstacle configuration. The first object was a methacrylate disk with a cylindrical vacuole 3 mm in diameter and 4 mm in height, which yielded stable internal PD activity at 13 kV. The second object was a twisted pair of conductors that generated surface PD at 10.3 kV.

3. RESULTS

Fig. 2 and Fig. 3 present the normalized average frequency spectrum obtained from the FFTs of the 200 signals recorded for each type of PD and obstacle configuration. In both figures, the black colored signal represents the average of the measurements performed without metallic obstacles around the PD source, while the colors indicate the cases with the different obstacle configurations. The low intensity in the frequency bands above 600 MHz stands out in all configurations and types of PD, with the exception of the 1200 MHz and 1350 MHz bands, frequencies used in amateur radio and aeronautical radionavigation. In these frequencies, commonly detected in the Santiago area where the measurement laboratory is located, the impact of metallic obstacles is lower, as shown in Fig. 2 and Fig. 3.

The lower graph in Fig. 2 shows the spectrum below 600 MHz corresponding to the measurements with the disk (internal PD), where significant differences between the signals with obstacles and those without obstacles can be seen. The configuration with cylindrical obstacles (blue signal) shows significant amplitude increases below 100 MHz and in the 300-400 MHz range. Rectangular obstacles (red signal) have their most pronounced effect at amplitude increases between 100 and 200 MHz. In the bottom plot of Fig. 3, which shows the FFTs of surface discharges below 600 MHz, prominent increases are observed between 150 and 300 MHz for the rectangular obstacle configuration (signal in purple) and around 100 MHz for the cylindrical obstacles (signal in green). This analysis, based on the normalized averages of the FFTs of the recorded signals, allows us to identify in which frequency bands the largest amplitude increases are observed, although it does not provide information on the number of PDs exhibiting this behavior. Inspired by the PRPD method, the graph in Fig. 4 is proposed, which shows not only the increase in signal amplitude (expressed as the quotient between the normalized FFTs with and without obstacles), but also the number of repetitions of that event. The clusters in Fig. 4 highlight the frequency bands where relative gain increases occur recurrently. Among these are the bands identified by the average FFT analysis, in addition to others not detected in the plots of Fig. 2 and Fig. 3. Thus, the plot proposed in Fig. 4 constitutes a more robust tool for the detection of relevant frequency bands in this analysis.

The normalization used to obtain the clusters in Fig. 4 is based on the following calculation procedure:

$$\widetilde{M}_O = \frac{M_O(i)}{P_{m\acute{a}x}(i)} \quad (1)$$

$$G = \frac{\widetilde{M}_O}{\widetilde{M}_S} \quad (2)$$

Donde

M_O is the $n \times i$ – dimensional matrix of the FFT of the signals captured with an obstacle configuration and a PD type.

\widetilde{M}_O is the matrix M_O where each of the signals i has been normalized with respect to its value.

$P_{m\acute{a}x}$ is the maximum amplitude of the i -th signal of the matrix M_O .

\widetilde{M}_S is the average normalized FFT of the unobstructed case for a PD type.

G is the $n \times i$ dimensional matrix of gain or quotient between the FFT of the normalized signal i and \widetilde{M}_S .

i is the number of signals recorded for each obstacle configuration and PD type.

n is the number of points that make up the FFT of each recorded signal.

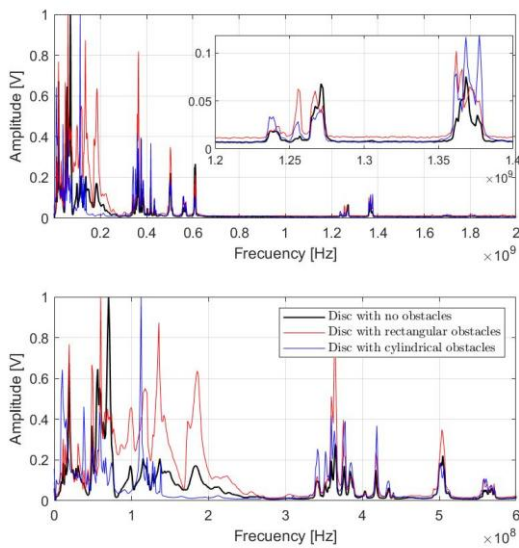


Fig. 2 Frequency spectrum of internal PD UHF signals captured with different obstacle environments.
 Source: own elaboration.

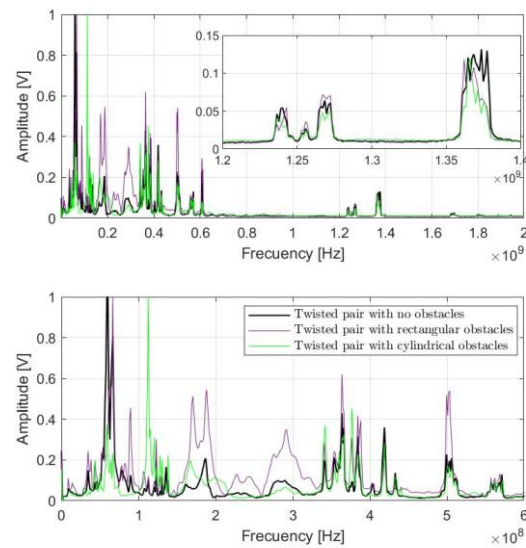


Fig. 3 Frequency spectrum of surface PD UHF signals captured with different obstacle environments.
 Source: own elaboration.

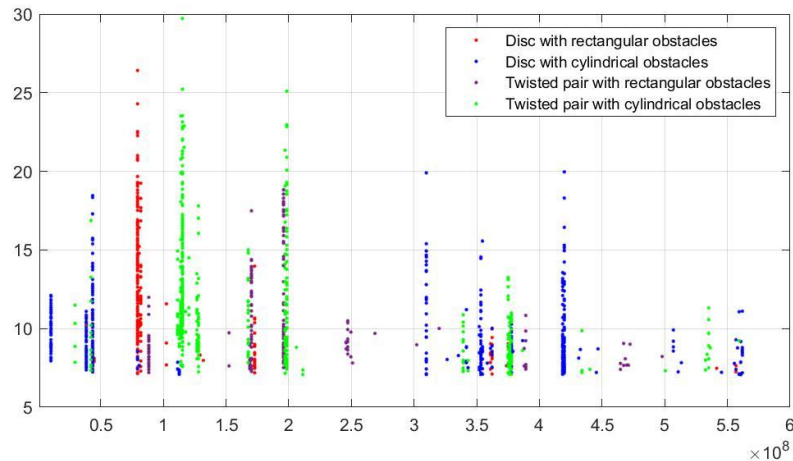


Fig. 4 Normalized gains of all tested configurations.
Source: own elaboration.

The data of the four G matrices obtained are shown in the plot in Figure 4, whereby each point indicates the quotient between the normalized value of one of the i recorded signals and the normalized value of the unobstructed signal for PDs of the corresponding type. The colors of the average FFT plots have been maintained for clarity and easy interpretation. In addition, a minimum limit of 7 pu for the significant gains was established in the construction of the graph to maintain control over the density of the clusters and an appropriate individualization of the frequency bands where the effect of the obstacle configurations is more intense.

The distribution of the clusters is indicative of the existence of clear and specific effects of the different configurations of obstacles on the PD sources analyzed, coming from the constructive interference between the signal emitted by the PD source and the signal reflected in the metallic obstacles arranged. Table 1 shows the clearly differentiated fringes with a number of events over 10% of the total. These data on the behavior of the constructive interference provide a clear background that any interference pattern to be constructed for a given measurement environment should focus on the frequencies that see their amplitude increased with respect to the case without obstacles, since the evidence collected shows that they are specific to each combination of PD source and obstacle configuration.

One of the cases with a significant concentration of events corresponds to the 115 MHz band for the case

of surface PD and cylindrical obstacles, in green. In this band more than 50% of the upper gains of the recorded signals are concentrated, not finding another frequency band so notorious where the case of surface PD and cylindrical obstacles appears alone. At 196 MHz and 377 MHz the points are accompanied by data from the other combinations of PD and obstacle configuration. Similar is the behavior of the gains in the case of internal PD and rectangular obstacles, where most of the maximum gains occur for a defined frequency band of 79 MHz, appearing again important gains at 170 MHz and 377 MHz, but coinciding with other types of discharges and obstacles.

The case of internal discharges with rectangular obstacles is the most distributed, presenting at least four frequency bands equally outstanding and in solitary, that is, where only this combination causes significant increases in the amplitude of the signal with obstacles. These bands are distributed throughout the spectrum under analysis, appearing at 10 MHz, 40 MHz, 309 MHz and 420 MHz.

Finally, the gains calculated on the basis of the records obtained with surface discharges and rectangular obstacles are the most dispersed, less intense and recurrent, with only two frequency bands appearing alone around 88 MHz and 250 MHz, with a low concentration of events close to 20% each. The other frequencies in which it appears always coincide with amplitude increase phenomena caused by other combinations.

Table 1: Summary of frequency bands of each PD source and obstacle configuration

	10 MHz	40 MHz	79 MHz	88 MHz	115 MHz	128 MHz	170 MHz	196 MHz	247 MHz	309 MHz	339 MHz	353 MHz	377 MHz	420 MHz
Internal PD with rectangular obstacles (red)			●				●						●	
Internal PD with cylindrical obstacles (blue)	●	●								●		●	●	●
Surface DP with rectangular obstacles (purple)				●			●	●	●					
Surface DP with cylindrical obstacles (green)					●	●	●	●			●		●	

4. CONCLUSIONS

The evidence gathered supports that the presence of grounded metallic obstacles with high geometric symmetry defines specific frequency bands where the amplitude increases of the frequency components of the signals emitted by the PDs are maximal. However, the most prominent variations were observed in the VHF region of the electromagnetic emissions, picked up by the Vivaldi antenna despite being tuned for signals in the UHF range. This underlines the need to use antennas tuned to different frequencies to achieve a more complete characterization of the effect of metallic obstacle configurations on the frequency spectrum of the recorded signals.

In addition, it is crucial to extend the trials to include both surface and internal PD combinations as well as other obstacle configurations. In this first set of tests, the symmetrical arrangement of obstacles increases the probability of observing frequency bands with constructive interference; however, distributing the obstacles randomly, while maintaining the obstacle geometry, could change the frequency bands detected. Even so, it is expected that any new obstacle configuration will reveal areas of the spectrum with evidence of constructive interference from electromagnetic emissions, allowing the development of techniques to identify and filter reflected signals. This will facilitate more accurate analysis of PD behavior based on UHF signals emitted directly from the source. This filtering of processed signals could be implemented in controlled measurement

environments, without movement of personnel or equipment, such as generator rooms in power plants, AIS or GIS substations, or specialized laboratories.

REFERENCES

- [1] Kreuger, F. Partial Discharge Detection in High-Voltage Equipment; Butterworths: Dayton, OH, USA, 1989.
- [2] Kuffel, E.; Zaengl, W.S.; Kuffel, J. High Voltage Engineering Fundamentals; Butterworth-Heinemann: Oxford, UK, 2000.
- [3] P. Morshuis, “Degradation of solid dielectrics due to internal partial discharge: some thoughts on progress made and where to go now,”IEEE Trans.Dielectr. Electr. Insul.,vol. 12, pp. 905–913,Oct. 2005.
- [4] Shibuya, Y.; Matsumoto, S.; Tanaka, M.; Muto, H.; Kaneda, Y. Electromagnetic waves from partial discharges and their detection using patch antenna. IEEE Trans. Dielectr. Electr. Insul. 2010, 17, 862–871
- [5] A. J. Reid, M. D. Judd, R. A. Fouracre, B. G. Stewart, D. M. Hepburn, “Simultaneous measurement of partial discharges using IEC60270 and radio-frequency techniques,”IEEE Trans.Dielectr. Electr.Insul.,vol.18, pp.444-455, April 2011.
- [6] S. Coenen, S. Tenbohlen, S. M. Markalous, T. Strehl, “Sensitivity of UHF PD measurements in power transformers,”IEEE Trans.Dielect. Electr. Insul.,vol.15, pp.1553-1558, Dec. 2008.

- [7] Albarracín, R.; Ardila-Rey, J.A.; Mas'ud, A.A. On the Use of Monopole Antennas for Determining the Effect of the Enclosure of a Power Transformer Tank in Partial Discharges Electromagnetic Propagation. *Sensors* 2016, 16, 148.
- [8] C. Boya, M. V. Rojas-Moreno, M. Ruiz-Llata and G. Robles, "Location of partial discharges sources by means of blind source separation of UHF signals," in *IEEE Transactions on Dielectrics and Electrical Insulation*, vol. 22, no. 4, pp. 2302-2310, August 2015, doi: 10.1109/TDEI.2015.004482.
- [9] IEC 60270: High-voltage test techniques - Partial discharge measurements. International Electrotechnical Commission, 3rd ed., 2000.
- [10] Albarracín Sánchez, Ricardo & Robles, Guillermo & Martínez-Tarifa, Juan & Ardila-Rey, Jorge. (2015). Separation of sources in radiofrequency measurements of partial discharges using time-power ratio maps. *ISA Transactions*. 58. 10.1016/j.isatra.2015.04.006.
- [11] A. Cavallini, M. Conti, A. Contin, G. C. Montanari, and G. Pasini, "An integrated diagnostic tool based on PD measurements," *Proc. Electr. Insul. Conf.*, pp. 219–224, 2001.
- [12] R. Schwarz, T. Judendorfer, and M. Muhr, "Review of partial discharge monitoring techniques used in high voltage equipment," *Annu. Rep. - Conf. Electr. Insul. Dielectr. Phenomena, CEIDP*, pp. 400–403, 2008.
- [13] M. D. Judd, L. Yang, and I. B. B. Hunter, "Partial discharge monitoring for power transformers using UHF sensors part 1: Sensors and signal interpretation," *IEEE Electr. Insul. Mag.*, vol. 21, no. 2, pp. 5–14, Mar. 2005.
- [14] S. M. K. Azam, M. Othman, H. A. Illias, T. Abdul Latef, M. Tariqul Islam, and M. Fadzil Ain, "Ultra-high frequency printable antennas for partial discharge diagnostics in high voltage equipment," *Alexandria Eng. J.*, vol. 64, pp. 709–729, Feb. 2023.
- [15] M. Wu, H. Cao, J. Cao, H. L. Nguyen, J. B. Gomes, and S. P. Krishnaswamy, "An overview of state-of-the-art partial discharge analysis techniques for condition monitoring," *IEEE Electr. Insul. Mag.*, vol. 31, no. 6, pp. 22–35, Nov. 2015.
- [16] H. Jahangir, A. Akbari, P. Werle, and J. Szczechowski, "UHF PD measurements on power transformers-advantages and limitations," *IEEE Trans. Dielectr. Electr. Insul.*, vol. 24, no. 6, pp. 3933–3940, Dec. 2017.
- [17] F. Yang, C. Peng, Q. Yang, H. Luo, I. Ullah, and Y. Yang, "An UWB printed antenna for partial discharge UHF detection in high voltage switchgears," *Prog. Electromagn. Res. C*, vol. 69, no. October, pp. 105–114, 2016.
- [18] J. Liang, C. C. Chiau, X. Chen, and C. G. Parini, "Study of a printed circular disc monopole antenna for UWB systems," *IEEE Trans. Antennas Propag.*, vol. 53, no. 11, pp. 3500–3504, Nov. 2005.
- [19] O. Haraz and A.-R. Sebak, "UWB Antennas for Wireless Applications," in *Advancement in Microstrip Antennas with Recent Applications*, InTech, 2013.
- [20] H. Elkamchouchi, M. Mahmoud, T. ElNozahy, and I. Aly, "Theoretical and practical analysis of the cockroach antenna," *Natl. Radio Sci. Conf. NRSC, Proc.*, 2008.
- [21] L. A. M. M. Nobrega, G. V. R. Xavier, M. V. D. Aquino, A. J. R. Serres, C. C. R. Albuquerque, and E. G. Costa, "Design and development of a bio-inspired uhf sensor for partial discharge detection in power transformers," *Sensors*, vol. 19, no. 3, pp. 1–16, 2019.
- [22] *IEEE Trans. Antennas Propag.*, vol. 60, no. 5, pp. 2536–2540, 2012.
- [23] T. Jiang, J. Li, Y. Zheng, and C. Sun, "Improved Bagging algorithm for pattern recognition in UHF signals of partial discharges," *Energies*, vol. 4, no. 7, pp. 1087–1101, 2011.
- [24] T. Ishikura, H. Muto, K. Wada, and N. Hosokawa, "Distinction of the partial discharge source in oil by two frequency correlation method," *Proc. Int. Conf. Cond. Monit. Diagnosis, C*. 2008, pp. 42–45, 2008.